OXFORD

Cerebral Cortex, 2022, 1–12
https://doi.org/10.1093/cercor/bhac415
Original Article

Brainnetome atlas of preadolescent children based on anatomical connectivity profiles

Wen Li[1,2], Lingzhong Fan[1,2,3,4], Weiyang Shi[1,2,3], Yuheng Lu[1,2,3], Jin Li[1,2], Na Luo[1,2], Haiyan Wang[1,2], Congying Chu[1,2], Liang Ma[1,2,3], Ming Song[1,2], Kaixin Li[1], Luqi Cheng[5,6], Long Cao[7], Tianzi Jiang[1,2,3,4,6,*]

[1]Brainnetome Center, Institute of Automation, Chinese Academy of Sciences, 95 Zhongguancun East Road, Beijing 100190, China,
[2]National Laboratory of Pattern Recognition, Institute of Automation, Chinese Academy of Sciences, 95 Zhongguancun East Road, Beijing 100190, China,
[3]School of Artificial Intelligence, University of Chinese Academy of Sciences, 95 Zhongguancun East Road, Beijing 100190, China,
[4]Center for Excellence in Brain Science and Intelligence Technology, Institute of Automation, Chinese Academy of Sciences, 95 Zhongguancun East Road, Beijing 100190, China,
[5]School of Life and Environmental Sciences, Guilin University of Electronic Technology, No.1 Jinji Road, Qixing District, Guilin 541004, China,
[6]Research Center for Augmented Intelligence, Zhejiang Lab, Kechuang Avenue, Zhongtai Sub-District, Yuhang District, Hangzhou 311100, China,
[7]Key Laboratory for NeuroInformation of Ministry of Education, School of Life Science and Technology, University of Electronic Science and Technology of China, No.4, Section 2, North Jianshe Road, Chengdu 610054, China

*Corresponding author: Brainnetome Center, Institute of Automation, Chinese Academy of Sciences, Beijing 100190, China. Email: jiangtz@nlpr.ia.ac.cn

During the preadolescent period, when the cerebral thickness, curvature, and myelin are constantly changing, the brain's regionalization patterns underwent persistent development, contributing to the continuous improvements of various higher cognitive functions. Using a brain atlas to study the development of these functions has attracted much attention. However, the brains of children do not always have the same topological patterns as those of adults. Therefore, age-specific brain mapping is particularly important, serving as a basic and indispensable tool to study the normal development of children. In this study, we took advantage of longitudinal data to create the brain atlas specifically for preadolescent children. The resulting human Child Brainnetome Atlas, with 188 cortical and 36 subcortical subregions, provides a precise period-specific and cross-validated version of the brain atlas that is more appropriate for adoption in the preadolescent period. In addition, we compared and illustrated for regions with different topological patterns in the child and adult atlases, providing a topologically consistent reference for subsequent research studying child and adolescent development.

Key words: anatomical connectivity; Brainnetome atlas; development; diffusion magnetic resonance imaging; preadolescent child.

Introduction

The preadolescent period is a critical time in the transition from childhood to adolescence. The brains of preadolescent individuals are usually >90% of the size of an adult brain (Dekaban and Sadowsky 1978), the total surface area is approaching peak (Bethlehem et al. 2022), and macroscale cortical organization gradients shift continuously in the period (Dong et al. 2021). However, the most advanced cognitive abilities still undergo substantial changes during development until adolescence or even adulthood (Bassett et al. 2011; Gu et al. 2015). The structure, function, and connectivity of the brain have already undergone dynamic changes throughout earlier childhood with each region across the whole brain having a unique neurophysiological developmental pace. These differences are particularly evident in the contrast between the primary cortex and association cortex (Casey et al. 2005; Sydnor et al. 2021). Neuroanatomically, brain areas, especially the higher-order integrative association areas compared with the primary cortex, show a pronounced tendency to increase or decrease in number of synapses, neuronal density, number of dendrites, and white matter volume, thereby forming the basis for complex cognitive processing (Buckner and Krienen 2013).

Brain atlases that are based on structural connectivity can reveal the interaction between parcels, reflect a biologically meaningful pattern, and provide fundamental insights into the organization and function of the human brain (Eickhoff et al. 2018). In the past decade, extensive developments in and applications of high-field scanners allowed researchers to gain a deeper understanding of the brain microstructure. Diffusion magnetic resonance imaging (dMRI) is an in vivo neuroimaging technique that enables researchers to reconstruct the tractography of white matter fiber tracts in the brain. Because it is sensitive to the heterogeneity in long-range connections, structural connectivity-based dMRI data have been extensively used to parcellate the human brain (Johansen-Berg et al. 2005). In addition, to a certain extent, structural connections constrain the functional diversity of brain regions (Passingham et al. 2002). Research also indicated that structural connectivity can predict functional activations (Saygin et al. 2016). Because they provide information at the intersection between microstructural and connectivity maps, atlases based on structural connectional architecture provide researchers with robust and biologically plausible anatomical parcels and supply the foundation for brain research.

The construction of the structural and functional networks that engender multiple complex cognitions is not complete in children's brains (Betzel et al. 2014). In general, there is a tendency

Received: July 22, 2022. **Revised:** September 17, 2022. **Accepted:** September 18, 2022

for brain function to progress from general to refinement throughout development (Barrett 2012). In early life, some subregions that are clearly divided in adults remain undifferentiated in children's brains, and the boundaries between functional areas tend to become progressively more refined and distinct as development progresses (Qin et al. 2012; Cadwell et al. 2019). Thus, there is no doubt that significant differences exist in regional patterns between children and adults. However, until now, most atlases have focused on adults. The few existing child atlases, while providing critical a priori knowledge of brain anatomy for later studies of children, are mostly templates composed of structural brain MR images (Jelacic et al. 2006; Fonov et al. 2009, 2011) and do not contain partitioning information or contain insufficiently detailed partitions (Molfese et al. 2021; Zhu et al. 2021). Whole-brain parcellation schemes based on structural connectivity information from age-specific children have not been made, and systematic comparisons of the parcellation patterns of the whole brain between childhood and adulthood have not been investigated in studies involving brain parcellation. Therefore, a child brain atlas for age-specific children with finer divisions should receive significant interest and be helpful for researchers.

To fill this critical gap, we have completed a new children's version of the Brainnetome brain atlas for preadolescent children. By taking advantage of an existing longitudinal dataset, in this study we were able to investigate variations in the parcellation patterns of the participants after 2 years of growth. To reveal the variation in the timing of regionalization in different brain regions in development, we compared the differences between the child and adult atlases based on their arealization and structural connections patterns. In addition, we explored the asymmetric patterns of regionalization in the left and right hemispheres for both the child and adult atlases. Compared with conventional MRI-based child atlases, the new children's version of the Brainnetome brain atlas not only provides finer partitioning, but also a structured connection pattern for each area. This new age-specific atlas for children should assist in future research into whether children have abnormal brain development as well as aiding in interventional treatments of early psychosis.

Materials and methods

Participants and image acquisition

The primary dataset used in this work was from a longitudinal multisite project, the adolescent brain cognitive development (ABCD) study. The brain scan images from 60 healthy participants (age: 9–10, 30 males) were collected on 3 tesla (T) Siemens Prisma scanner platforms and passed ABCD's extensive quality control. Both the baseline scans imaging of the same participants and the 2 years follow-up scan images were included in the parcellation process. None of the subjects included in this study had suffered from traumatic brain injury or any mental disease. All participants and their parents provided verbal and written consent/assent.

The 3D T1-weighted magnetization-prepared rapid acquisition gradient echo scan was achieved using an isotropic voxel resolution of $1 \times 1 \times 1$ mm^3, field of view (FOV) of 256×256 mm^2, and flip angle of 8°. The 3D T2-weighted fast spin echo with variable flip angle scan was achieved using the same voxel resolution and FOV as the T1-weighted scan. They were both used to perform registration between the multimodal data.

The diffusion imaging scan was achieved with high angular resolution, multiple b-values ($b = 500$ s/mm^2 (6-dirs), $b = 1{,}000$ s/mm^2 (15-dirs), $b = 2{,}000$ s/mm^2 (15-dirs), and $b = 3{,}000$ s/mm^2 (60-dirs)), flip angle of 90°, isotropic voxel resolution of $1.7 \times 1.7 \times 1.7$ mm^3 and FOV of 240×240 mm^2. The diffusion weighted images were acquired to identify the white matter tracts and measure the diffusion rate (Casey et al. 2018).

HCP-D dataset (Lifespan Human Connectome Project in Development) was used to supplement the data for other age groups of young people. The HCP-D Release 1.0 includes scan images from 655 subjects (323 males, age 5–21) acquired at 4 sites across the United States. The T1w scans were acquired using magnetization-prepared rapid gradient-echo (MPRAGE) (Van der Kouwe et al. 2008) sequence with a resolution of 0.8 mm, sagittal FOV of $256 \times 240 \times 166$ mm, and flip angle of 8°. The diffusion protocol involved sampling 185 directions on 2 shells of $b = 1{,}500$ and 3,000 s/mm^2 along with 28 $b = 0$ s/mm^2 images at a resolution of 1.5 mm and FOV of 210×210 mm^2 (Harms et al. 2018).

Data preprocessing

The ABCD dataset preprocessing process for the T1 and T2 weighted structural data included removing non-brain tissue, segmenting the gray and white matter, and parcellating the cerebral cortex to obtain the initial parcels based on the Desikan–Killiany (DK) atlas (Desikan et al. 2006) using FreeSurfer v6.0 (http://surfer.nmr.mgh.harvard.edu/). Next, individual structural images were registered to the asymmetric National Institutes of Health pediatric database (NIHPD) pre-to-early puberty (7–11 years) template (Fonov et al. 2009, 2011) using linear affine registration and nonlinear deformations of the SPM12 (https://www.fil.ion.ucl.ac.uk/spm/software/spm12/), and then averaged to build the group template. The resulting transformation matrixes were used to perform transformations of the template space and individual T1 space. Utilizing the method in Fan et al. (2016), the obtained initial parcels in each subject were then used to create population probability maps that were binarized using a threshold of 25% to obtain the initial regions of interest (ROIs) for a more refined parcellation. The FMRIB Software Library (FSL) (http://www.fmrib.ox.ac.uk/fsl/) was used to correct the head motion and eddy currents of the diffusion MRI data. The T1-weighted image of each subject was co-registered to the corresponding non-diffusion-weighted images using SPM12, and then the inverse transformation was performed to transform the initial ROIs into seed masks of the diffusion space.

For the HCP-D dataset, the minimal preprocessing pipeline was performed (Glasser et al. 2013; see https://github.com/Washington-University/Pipelines) to preprocess the structural and diffusion MRI data. To facilitate comparative analysis between cohorts, the subjects were divided into 4 age groups, preadolescence (8–10 years), early-adolescence (11–14 years), middle-adolescence (15–17 years), and late-adolescence (18–21 years; Hagan et al. 2017). Similarly, the initial parcels for each age group were obtained after parcellation using FreeSurfer. The diffusion data preprocessing included normalizing the $b0$ intensity, eddy current correction, echo planar imaging correction, head motion correction, and registering diffusion data to structural space.

Parcellation pipeline

First, FSL's BEDPOSTX was employed to estimate the orientation and the associated uncertainties of the fibers in each voxel within the brain mask. Next, to estimate the connectivity probability between voxels in the whole brain, for every voxel in each seed mask, 5,000 streamline fibers were sampled using the FSL package (Behrens et al. 2007) with the angle threshold and the number of steps per sample set to 0.2 and 2,000, respectively. The number

of streamlines entering each voxel was then divided by 5,000 to normalize the results across the whole brain. After applying a threshold of 2/5,000 (Johansen-Berg et al. 2007; Makuuchi et al. 2009) to reduce the number of false positive samples, the whole-brain connectivity profiles from the probabilistic tractography were down-sampled to 5-mm isotropic and transformed into an $N \times M$ anatomical connectivity matrix in which N was the number of voxels in each seed mask and M was the number of voxels in the whole brain. Then the anatomical connectivity matrix was used to generate an $N \times N$ symmetric cross-correlation matrix. The value in the cross-correlation matrix is the correlation between the connectivity profiles of the voxels of the seed ROI.

Spectral clustering was used to generate 2–10 clusters using the cross-correlation matrix as features. Maximum probability maps were created across all the subjects for the whole brain. However, when matching subregions based on the overlap rate of voxels between subregions, some smaller subregions were mislocated and labeled to the wrong ROI. In view of this limitation, the similarity of fiber connection patterns was also taken into consideration. Because there was no previous child brain atlas with a sufficiently fine parcellation pattern of the whole brain, the 72 major white matter tracts were applied as target areas in each subject. These tracts were obtained by segmenting the white matter tracts in fields of fiber orientation distribution function peaks using a fully convolutional neural network (Wasserthal et al. 2018). The steps for building the fiber connection matrix were the same as described previously. The mislabeled subregions were re-labeled based on the similarity of their fiber connection patterns. The integrated pipeline of the parcellation is shown in Fig. 1.

For each ROI, the appropriate number of partitions was carefully selected. Since structure, function, and connectivity change throughout the entire human lifespan, the brain parcellation patterns should not be the same in children and adults. The number of partitions of the brain regions that are more variable during individual development was carefully and thoughtfully confirmed. Then, the topological consistency (TC) inside each subregion, the individual consistency (IC) of the connectivity patterns between subjects, and the partition consistency (PC) between ages were all taken into account when determining the number of clusters of each ROI. The silhouette coefficient (SI; Rousseeuw 1987), which measure how similar an object is to its own cluster compared to other clusters, was used to measure the TC. A higher mean SI for all voxels in the ROI indicates lower intra-regional dissimilarity and higher inter-regional dissimilarity. The Dice index (Dice 1945), normalized mutual information (NMI) index (Danon et al. 2005; Lancichinetti et al. 2009), and Cramer's V (CV; Cramér 1999) were all used to measure the IC. The reproducibility was evaluated using cross-validation (Fan et al. 2016). The consistency of the cluster partition patterns across the 2 data collections was also taken into consideration as an important reference for deciding the final partition number and was also measured by the Dice index. These indexes were then normalized and compiled into an aggregate index that was used to determine the final number of partitions for each ROI, with higher local peaks in the aggregated index suggesting a potentially better partitioning pattern. The brain areas in which the children had a DN of partitions from the adult atlas all belonged to the association cortex. To determine the number of partitions for these areas, we not only needed to depend on the performance of each index but also to integrate information about the structural and functional changes in the development of these areas. By taking all the indexes described above into consideration, the most proper number for each ROI was determined for the children.

Comparison of different age groups

The partition patterns of each ROI were compared between the baseline group and the follow-up group of children and between the baseline children and the adults. Based on the partitioning patterns, the children's brain ROIs were divided into 2 groups. Specifically, ROIs with the same number of subregions as the adult partition were termed same-number (SN) ROIs, and ROIs with different patterns between the children and adults were named DN (different-number) ROIs. Importantly, just because an ROI was in the SN group did not mean that the structure and function of this ROI had not changed during the developmental stage from childhood to adult but simply indicated that the changes in structural connectivity were not sufficient to drive changes in the regionalization patterns even if the function of each subdivision of the package was reorganized during development.

The connectivity patterns of the ROIs in the DN group were compared between the children and adults using their connection fingerprints (Mars et al. 2016). The seed areas of the connection fingerprints were each parcel in the ROIs from the DN group, whereas the target areas of connection fingerprint were all the parcels in the ROIs from the SN group. The probabilistic fiber tracking process was the same as mentioned previously. After removing the false positive connections (Roberts et al. 2017), the connection matrix was obtained. After normalization, the matrices were averaged and thresholded to a group matrix that only retained fiber connections shared by >75% of the subjects. Finally, the connectivity pattern for each ROI was expressed as separate fingerprints and was used to determine the correspondence between the child and adult labels.

The nomenclature of each parcel in each ROI was mainly based on anatomical and modified cytoarchitectonic descriptions, as mentioned in (Fan et al. 2016), and the label correspondences were based on both the overlap of each voxel and the overlap of its structural connections. After naming all parcels, the connection matrix with the whole-brain parcel as seed and the whole brain as target was constructed as above. The sum of the connection pattern similarities and voxel overlaps of the parcels in each ROI were calculated to compare the parcellation patterns between the 2 age groups of the children as well as between the children and adults. To limit the data to between 0 and 1, both the similarity and overlap values were reduced by half. The significance of the comparison of the voxel overlap was performed by a paired t-test using Matlab. In addition, the voxel overlap of the parcels in Yeo's (Yeo et al. 2011) 7 networks was also calculated.

Asymmetry of the left and right hemispheres

To observe changes in the tendency toward lateralization of the brain from childhood to adulthood, the parcellation patterns of the left and right hemispheres were assessed for consistency between the hemispheres. Here, areas in the right hemisphere were aligned to the corresponding area in the left hemisphere after the coordinates were flipped using FSL; and then the degree of consistency was measured by the amount of voxel overlap. Since the template we used was asymmetric, the flipping and alignment process may have introduced some bias, but on the other hand, this asymmetry reflects the asymmetry of the left and right hemispheres. The asymmetry of the atlases based on subjects from the baseline children in the HCP-D and from the adults in the HCP-YA were calculated separately. Comparison of

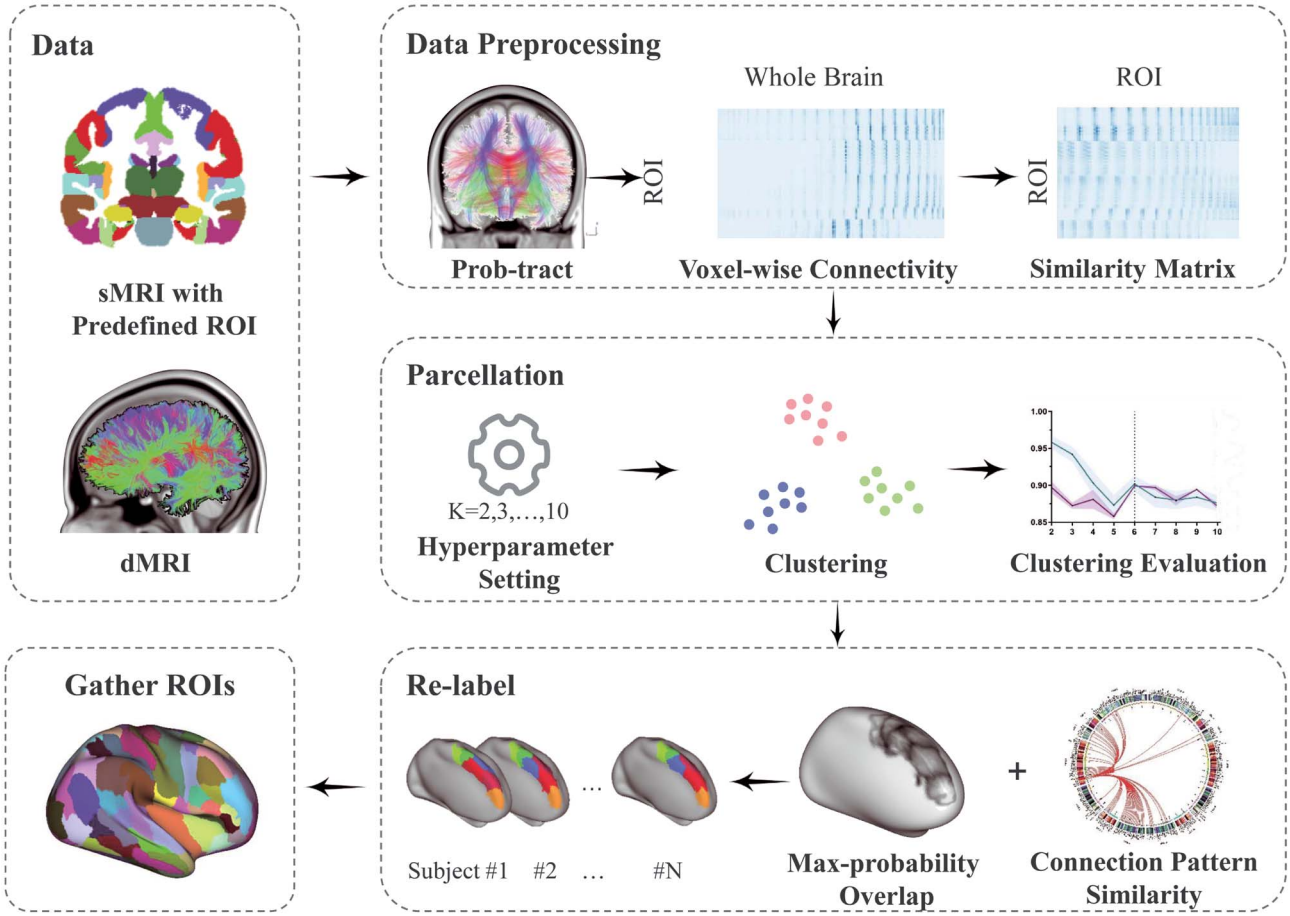

Fig. 1. The parcellation pipeline. The initial ROIs were produced by the FreeSurfer DK atlas using dMRI data. Then tractography-based connectivity and similarity matrices were computed for the subsequent clustering. After parcellating the data from all the individuals, a re-labeling process was performed to generate a group parcellation.

the symmetry between the child and adult atlases was performed by calculating the difference between them. For each region, the difference was defined as the adult left–right hemisphere topological symmetry minus the child left–right hemisphere topological symmetry after regressing out the differences in the regions of interest.

Results

Connectivity-based parcellation using the ABCD dataset

The cortical areas of the child atlas are shown in Fig. 2 and the subcortical regions are shown in Supplementary Fig. S1, see online supplementary material for a color version of this figure. Each hemisphere consists of 94 parcels in the cortex and 18 subcortical regions. The detailed partition numbers and names are in Supplementary Table S1, and the indexes for choosing the optimum number of partitions are listed in Supplementary Fig. S2 (see online supplementary material for a color version of this figure) and Supplementary Table S2. The parcellation numbers of the cortical ROIs in the child atlas that were identical to and different from the adult atlas were 72 and 22, respectively, in each hemisphere. The ROIs in the SN group of the child atlas included the middle frontal gyrus (MFG), inferior frontal gyrus (IFG), orbital gyrus (OrG), precentral gyrus (PrG), paracentral lobule (PCL), superior temporal gyrus (STG), middle temporal gyrus (MTG), fusiform gyrus (FuG), parahippocampal gyrus (PhG), posterior superior temporal sulcus (pSTS), inferior parietal lobule (IPL), precuneus (PCun), postcentral gyrus (PoG), medioventral occipital cortex (MVOcC), lateral occipital cortex (LOcC), and subcortical ROIs. Although these ROIs had the same number of partitions in the children and adults, this only indicates that the developmental changes were not sufficient to cause the original subdivisions to split or integrate to form new subdivisions. However, the function within each subregion may have shifted.

The ROIs in the DN group of the child atlas included the superior frontal gyrus (SFG), inferior temporal gyrus (ITG), superior parietal lobule (SPL), insular gyrus (Ins), and cingulate gyrus (CG). For these ROIs, we investigated in detail how each subregion in a given child's ROI corresponds to the subregions in the corresponding adults' ROI based on voxel overlap and the similarity in connectivity patterns (Fig. 3).

We previously described the details of the SFG partition pattern in childhood and obtained similar results in this current article in that the A9 area in childhood segregated to the A9m and A9l areas in adulthood (Li et al. 2022).

In the ITG, the rostral area 20 (A20r) was less variable during development and corresponds to the A20r area in the Brainnetome atlas. The intermediate lateral area 20 and caudolateral area 20 corresponded mainly to the regions with the same name in the adult atlas. Ventrolateral 37 in the child atlas consisted of the extreme lateroventral area 37 and ventrolateral area 37

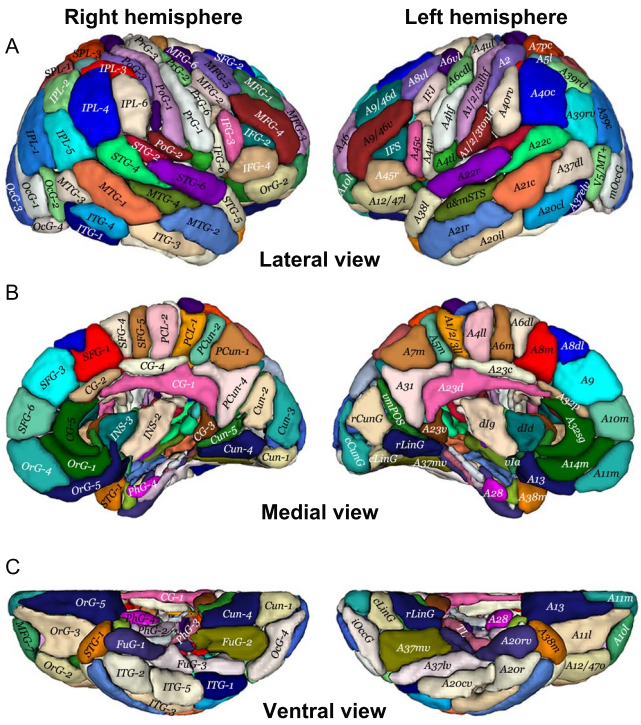

Fig. 2. The child Brainnetome atlas. In children, for ROIs that had the same partitioning pattern as adults, each subregion was given the same label and color as the adults; in contrast, in ROIs with dissimilar partition patterns, the labels and colors were found to correspond best to voxel overlap and connection patterns in the corresponding ROIs in the adults. The results are presented using ITK-SNAP software (Yushkevich et al. 2006).

in the adult Brainnetome atlas. Ventral area 20 consisted of the intermediate ventral area 20 and the caudoventral area 20 in the Brainnetome atlas. The latter 2 subregions in the child atlas appear to have undergone developmental re-segregation and integration to differentiate into more specific subregions in adulthood.

The SPL area was divided into 3 subregions. From the rostrum to the tail, the 3 subregions were the rostral SPL, which consists of the postcentral area 7 and rostral area 7; the lateral SPL, which consists of lateral area 5 and intraparietal area 7 (hIP3); and the caudal SPL, which consists of caudal area 7 and part of rostral area 7.

The Ins area was divided into 3 parts, that is, the posterior, dorsal, and ventral insulae. Previous researchers have used resting-state functional MRI (rfMRI) data to divide the insular lobe into 3 parts using a clustering approach, which yielded results that are in good agreement with our results (Deen et al. 2011). The posterior insula in the child atlas corresponds to regions that include the hypergranular, ventral dysgranular and granular, and dorsal granular insulae in the Brainnetome atlas. The dorsal insula in the child atlas corresponds to regions including the dorsal dysgranular and dorsal agranular insulae in the Brainnetome atlas. The ventral insula in the child atlas corresponds to the ventral agranular insula in the Brainnetome atlas.

The CG area was divided into 5 parts: anterior cingulate, anterior mid cingulate, posterior mid cingulate, dorsal posterior cingulate, and ventral posterior cingulate cortices. These respectively correspond to the subgenual area 32, pregenual area 32, caudal area 23, dorsal area 23, and ventral area 23 in the Brainnetome atlas.

Interestingly, the number of subregions in the child ROIs that belonged to the DN group was all fewer than the number in the corresponding area of the adult atlas. This suggests that further differentiation of the structural function of these brain regions occurred during development, thus leading to the splitting of ROIs into more specific subregions to participate in more subspecialized tasks.

The parcellation patterns of ROIs in the DN group using the HCP-D dataset

The parcellation patterns of the ROIs in the DN group are shown in Fig. 4 for 4 age groups, and the consistency between the 2 datasets of children are shown in Supplementary Fig. S3, see online supplementary material for a color version of this figure. For the 2 batches of data from ABCD, the 5-partition pattern of the ITG achieved 88.76% and 86.16% degree overlaps in the left and right hemispheres, respectively, and performed the best of almost all the intra-hemispheric partition models (the 2-partition pattern was not fine enough to be taken into account). However, between the different data sets at different ages, the ITG in the left hemisphere showed a better consistency for the 4-partition pattern than for the 5-partition pattern, whereas the ITG in the right hemisphere was good for either the 3- or 5-partition patterns. These results suggest that the structural connectivity patterns of the ITG change with age, perhaps affecting the regionalization patterns during development. However, the focus of this study was on preadolescent children, so the consistency between the 2 datasets of children was the main consideration. For the SPL and Ins areas, the 4-partition pattern and the 3-partition pattern achieved good performances across both ages and data sets. For the CG area in both the left and right hemispheres, the 5-partition model had the highest consistency between the 2 batches of data in ABCD compared with other patterns. However, if the data are extended to include the entire age range of development, the 4-partition pattern may be a better choice in the left hemisphere.

Comparison of atlas at different ages

The coincidence level between the cortical regions of the atlases of the children's baseline group and of the follow-up group are displayed in Fig. 5A. Given that the same subjects were used to build both atlases and that the time between the 2 image acquisitions was only about 2 years, most brain regions showed a relatively high overlap between the 2 age groups. Among the regions in the left hemisphere, the SFG, SPL, STG, MTG, PhG, and part of the subregion in the PrG showed relative variability between ages. In contrast, in the right hemisphere, only the MFG, PhG, and PrG showed variability between ages. Interestingly, the IPL in the different hemispheres exhibited different developmental trends between ages, with larger differences in the left hemisphere and fewer differences in the right hemisphere. This may be associated with the rapidly developing lateralized attentional and spatial perception abilities of children in this age range.

The levels of coincidence between the cortical regions of the atlases of the children and adults are displayed in Fig. 5B, and the subcortical regions are shown in Supplementary Fig. S4, see online supplementary material for a color version of this figure. Most of the regions with high consistency were in the primary and unimodal cortices and involve sensory and motor functions. In detail, the PCL is commonly thought to control motor and sensory functions of the lower limbs and perineum (Baker et al. 2018), the PoG is a significant brain region responsible for proprioception (Kropf et al. 2018), and the MVOcC participates in the visual information processing circuit. Although children and adults share

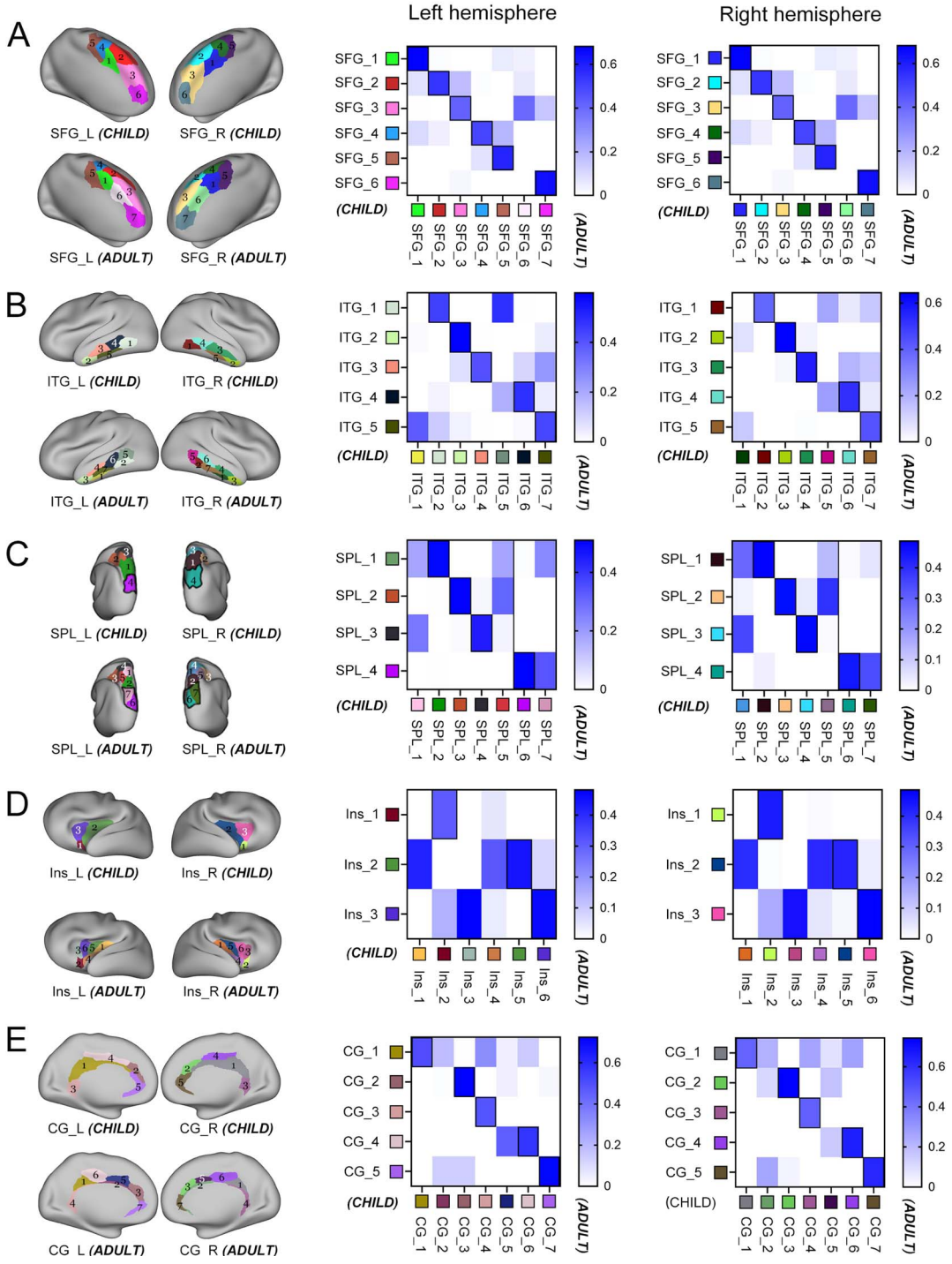

Fig. 3. Consistency in the relationship between subregions in ROIs in the DN group. In each panel, the left subplot is a display of the parcels of the ROIs in the child and adult atlas, respectively, the middle subplot is an overlap of the voxels and connections patterns of the parcels in that the ROI in the left hemisphere in the child's and adult's partition patterns, and the right subplots are the overlap of parcels in that ROI in the right hemisphere. The horizontal coordinates are for the adult subregions and the vertical coordinates are for the child subregions. The same color indicates the corresponding area. A) The parcellation pattern of the SFG area and the corresponding relations of each parcel of the SFG in the child and adult atlases. B) The parcellation pattern of the ITG area and the corresponding relations of each parcel of the ITG in the child and adult atlases. C) The parcellation pattern of the SPL area and the corresponding relations of each parcel of the SPL in the child and adult atlases. Note that parts of the initial ROIs of SPL obtained from FreeSurfer were located in the occipital lobe, which was circled in black solid circles in the figure. These regions were later corrected to the occipital lobe when nomenclature was performed. D) The parcellation pattern of the Ins area and the corresponding relations of each parcel of the Ins in the child and adult atlases. E) The parcellation pattern of the CG area and the corresponding relations of each parcel of the CG in the child and adult atlases.

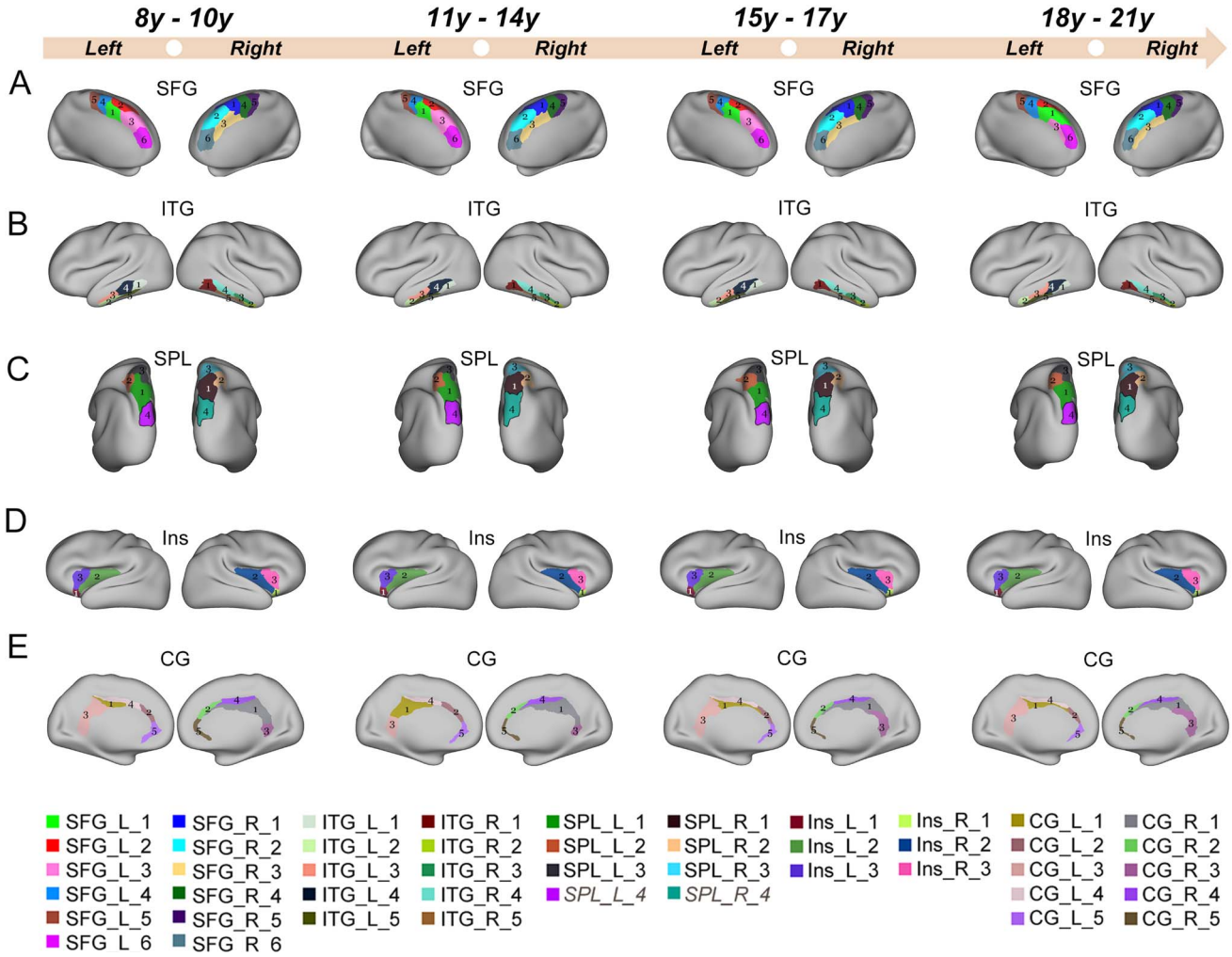

Fig. 4. Parcellation patterns of ROIs in the DN group and the degree of overlap within a data set and across different data sets. A), B), C), D), E) show the parcellation patterns of the SFG, ITG, SPL, Ins, and CG, respectively. From left to right, the parcellation pattern are from preadolescence, early-adolescence, middle-adolescence, and late- adolescence.

the same number of partitions in the OrG, part of the default network, the overlay rate is relatively smaller than other ROIs in SN ROIs group. Similarly in the STG and MTG, which are most commonly related to processing auditory information (Giraud and Price 2001) and encoding memory (Taing et al. 2021), also underwent relatively large changes in partition patterns during development. The above all belong to the higher-order, trans-modal association cortices, which mature later with a protracted plasticity compared to other regions in the unimodal cortices. It is worth noting that the SPL in both the left and right hemispheres showed considerable variation, implying that both sides of the SPL undergo relatively large changes during development from childhood to adulthood, although the timing of the changes may not be the same on the 2 sides. Because of differences between the atlases of the children and adults, the initial ROIs did not have a good correspondence, resulting in a generally low overlap for the subcortical regions. This low overlap is probably driven by the unrefined functions associated with subcortical regions.

To better illustrate the importance of creating a child atlas, the overlap levels between the baseline children and the follow-up children (C–C) and between the baseline children and adults (C–A) are exhibited in Fig. 5C. Compared with comparisons with adults, comparisons between children (C–C) had significantly more consistent results, with a regional mean overlap of 0.85, whereas the regional mean overlap was 0.53 for the C–A. In the comparison between the children's atlases, all the networks achieved an overlap rate of 0.85 or higher, except for the default network. In contrast, the overlap between the child and adult atlas was <0.8 for all networks and was particularly low for the ventral attention network and limbic network. On the one hand, this may be because comparisons between children were made using the same group of subjects, whereas comparisons between the children and adults were made with different subjects. On the other hand, this result also implies that changes in the structure and function of the developing child's brain lead to large-scale changes in partitioning patterns and suggests the irrationality of applying an adult atlas in child studies.

Asymmetry of the left and right hemispheres

The asymmetry of cortical regions of child atlas and adult atlas is illustrated respectively in Fig. 6A and B, in which darker colors indicate higher asymmetry. A comparison of atlas asymmetry in adults and children is shown in Fig. 6C, in which blue areas indicate an increase in asymmetry through development and orange indicates decreasing asymmetry. The asymmetry of the subcortical regions is shown in Supplementary Fig. S5, see online supplementary material for a color version of this figure. In general, the child and adult atlases shared similar asymmetry

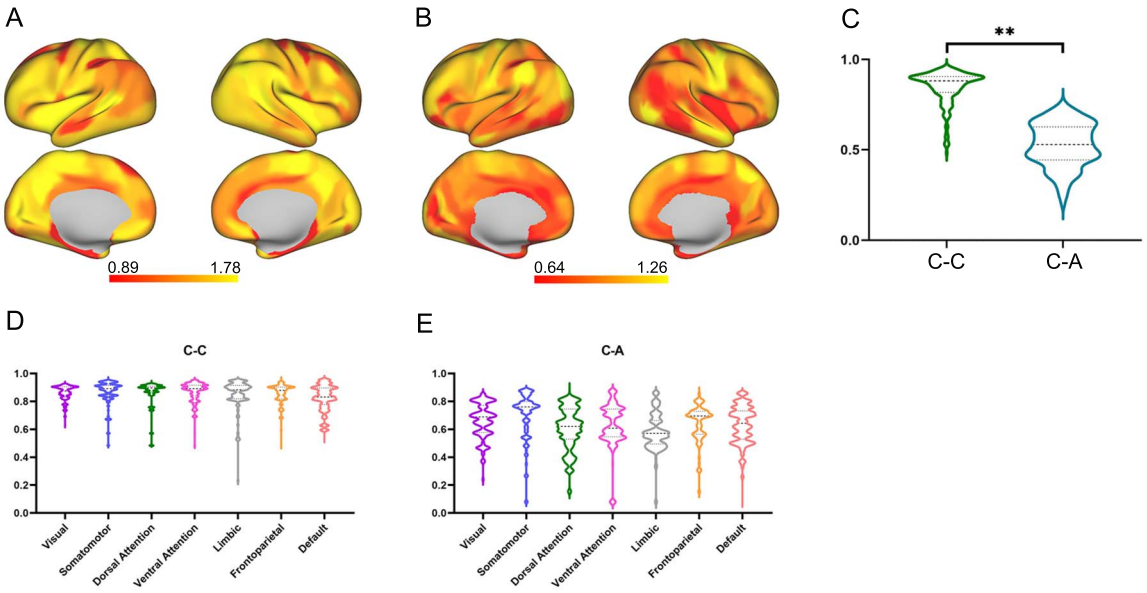

Fig. 5. Degree of overlap of the atlases for different ages. The reference parcellation pattern is from the children's imaging in the baseline scans. Darker colors indicate less overlap. A) Comparison of parcellation patterns in children of 2 age groups. B) Comparison of parcellation patterns between children and adults. C) ANOVA analyses of the degree of overlap between the child and adult atlases. Only significance with $P < 0.01$ is shown. D) ANOVA analyses of the overlap degree between the 2 age groups of children based on the Yeo network. E) ANOVA analyses of the overlap degree between the child and adult atlases based on the Yeo network.

patterns. More specifically, the PrG, PoG, STG, SPL, MVOcC, and medial OrG exhibited clear asymmetry between the left and right subregions. As seen in Fig. 6C, most regions showed asymmetry that increased with development. This was particularly evident in the MFG, SPL, IPL, STG, CG, and part of the Ins. Some regions, such as part of the PrG, LOcC, MTG, and the posterior part of the SFG, showed reduced asymmetry. The asymmetry in the parcellation patterns might arise from the asymmetry of the templates used or might be due to the structure and function of the lateralized brain. Changes in structure and function during development as well as the level of symmetry of the templates used for the child and adult atlases may have contributed to the changes in developmental asymmetry.

Discussion

In this study, we developed an innovative age-specific atlas of the child brain. Selecting age-specific subjects facilitated our ability to capture the topographical patterns of brain structure specific to each age group, and the longitudinal data allowed us to track changes in the developing brain of the same subject cohort more credibly. In line with previous studies, we found that the developmental trajectories of the ROIs across the whole brain are heterogeneous. When we compared the child and adult atlases, the primary cortex, including the sensory, visual, and motor cortexes, showed low variability between the children and adults in this study. In contrast, the association cortex, especially the multimodal association cortex, showed considerable topographic variability during development as well as significant variations in their connectivity profiles. For ROIs in the DN group, the progressive refinement and formation of sharp boundaries between the subregions, expressed as an increase in the number of partitions, could be considered as a projection of the transformation of subregion function from generalization to specialization (Cadwell et al. 2019). Interestingly, the trend that emerged when comparing the child atlas with the adult atlas,

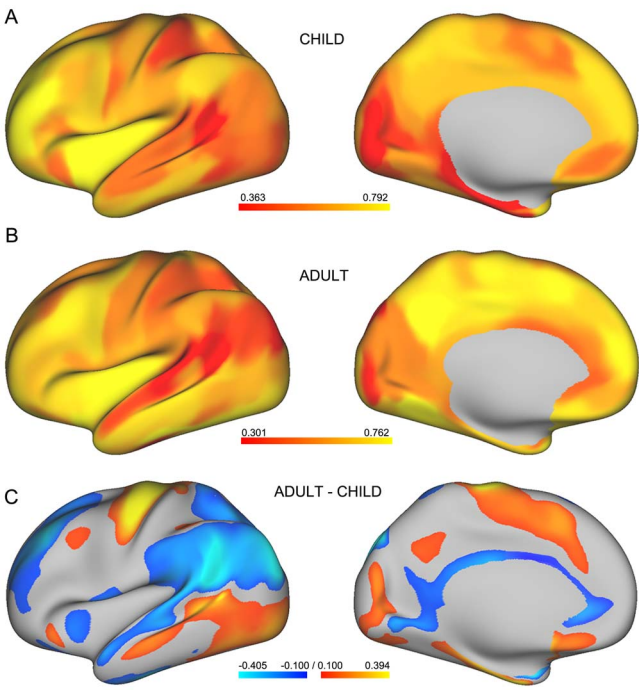

Fig. 6. Asymmetry between hemispheres. A) and B) respectively represent the symmetry of the child atlas and the adult atlas. Darker colors indicate low asymmetry. C) Change in symmetry during the development from childhood to adulthood. Blue indicates areas of increased asymmetry in development, whereas orange represents areas of increased symmetry. Only areas with absolute values >0.1 are displayed. To obtain a better contrast of the display, the range of values displayed in the 3 figures was limited to between 4% and 96% of the full value.

i.e. less variation in development in the unimodal cortex and greater variation in the multimodal cortex, did not appear when the 2 child age atlases were compared. This further indicates that

the structural reorganization of various brain regions does not occur simultaneously; instead changes in each area occur in its own time.

The differential changes in topographical patterns across brain areas are probably attributable to asynchronous structural changes during development. Cortical volume and cortical thickness both tend to increase in childhood and then decrease in adolescence. However, the timing of this tendency is regionally variable in that the primary areas show earlier peaks in volume and thickness than the higher-order association areas (Lenroot and Giedd 2006; Wierenga et al. 2014), suggesting that the structural and functional framework of the primary areas had already been established. The remodeling of gray and white matter continues into the third decade of life (Lenroot and Giedd 2006), hence the resulting arealization may continue into adulthood. In addition, rapid myelin changes occur during adolescence, with differences in timing in different brain areas (de Faria et al. 2021). These differences may directly contribute to changes in structural connectivity, constrain changes in functional connectivity, and ultimately affect the maturation of regionalization (Yakovlev et al. 1967; de Faria et al. 2021).

Interestingly, the IPL areas of the left and right hemispheres of the brain showed significant differences between the 2 age groups of children. Considering that the time interval between the 2 brain image acquisitions was about 2 years, it is interesting that even such a short period could cause a distinct difference between hemispheres from a regionalization perspective; in other words, this short period led to obvious changes in structurally connectivity. Previous studies showed that the parietal lobe undergoes a period of continuous high growth in childhood and that this process lays the foundation for the growth of children's language skills and the ability to understand spatial relations (Thompson et al. 2000). As part of a left-hemisphere-lateralized semantic system (Binder et al. 2009), the process of asynchronous inter-hemispheric regionalization in the IPL also suggests a lateralization of language functions during development. Children face increasingly more challenging information processing tasks that enhance their reading ability with respect to information and comprehension (Loveless 2020); this enhanced ability in turn promotes the development of brain physiological structures. Furthermore, this result implies the necessity for research that can lead to age-specific atlases, especially during childhood when brain structure and function are rapidly changing. An atlas made using subjects of multiple ages can confound subtle differences in development at different ages; such subtle differences are particularly critical in children's studies.

Regionalization patterns of ROIs in the DN group exhibited considerable variations between the atlases of the children and adults. The subregions with greater refinement reflect the growing maturity of the children's structures and functions. Among these ROIs, the ITG is a higher-order association area that is involved in processing visual information (Lafer-Sousa and Conway 2013) and exhibits a specific pattern of late maturity. It is also considered to be the most recent evolutionarily. According the functions of the ventrolateral area 37 and ventral area 20, segregation within these areas may potentially reflect a refinement of the function of the visual numeral response (Shum et al. 2013). The SPL is mainly involved with sensorimotor integration and spatial orientation (Gardner 2008). As a major component of the dorsal attention network, the borders of the SPL are systematically refined during development. During childhood, changes in individual topographic variability may herald further functional maturation (Cui et al. 2020), providing evidence for the rapid development of working memory and short term learning, which involve the SPL (Koenigs et al. 2009; Ossmy and Mukamel 2016). The 3 subregions in the insular lobe, posterior insula, dorsal insula, and ventral insula were involved in distinct functions. The first 2 subregions are further differentiated in adults to generate more specific subregions that may respond to more refined cognitive tasks or tasks that process sensory information (Cereda et al. 2002; Cerliani et al. 2012; Cloutman et al. 2012; Nomi et al. 2016; Ghaziri et al. 2017). As part of the limbic system, the CG is involved in many vital neural circuits and is considered a connecting hub for multiple functions (Jumah and Dossani 2019). A functional connectivity study indicated that the functions of the anterior cingulate subregions, which are associated with cognition, undergo considerable changes during childhood and adolescence and that each subregion matures at different times depending on the specific division of functions (Kelly et al. 2009). Longitudinal studies of these ROIs will make it easier to track the different maturation times of related functions, and to understand the underlying processes of microstructural maturation and developmental psychopathology.

The symmetry of the regionalization patterns between the left and right hemispheres showed similar patterns in the child and adult atlases. In both children and young adults, asymmetry of regionalization was consistently observed between the 2 hemispheres in the PrG, PoG, STG, SPL, MVOcC, and medial OrG areas, whereas the degree of asymmetry was relatively low in children. These asymmetries are supported by the structural basis of the brain. Previous research reported greater leftward thickness asymmetry patterns in the PrG (Luders et al. 2006) and significant leftward asymmetry patterns of the surface area of the PoG (Koelkebeck et al. 2014). Significant rightward asymmetry in the somatosensory motor area was also reported (Liang et al. 2021). The asymmetry in the frontal and occipital lobes may be attributable to geometric distortion of the brain hemispheres, termed the Yakovlevian anticlockwise torque, in which the right frontal region is often wider than the left and the left occipital pole is often wider than the right (Renteria 2012). The lateralization of the visual network may also be associated with the right-dominance of visual functions, as previously reported (Gracia-Tabuenca et al. 2018). In addition, as part of the higher language areas, the STG increasingly shows a leftward asymmetry in development and grows slowly with language learning process until it forms a pattern of intra-hemispheric language in adults (Tzourio-Mazoyer 2016). Hand preference is also associated with structural and functional asymmetries in language-processing structures, especially in the temporal lobe (Toga and Thompson 2003). Heschl's gyrus, which is located in the STG, is typically larger in right handers on the left side (Penhune et al. 1996) and may contribute to the asymmetry of the STG. The most pronounced region of developmental asymmetric growth between the left and right sides occurs in the parietal lobe, implying that aging brings structural and functional changes that promote an increasingly pronounced division of function between the left and right hemispheres of the parietal lobe. In the dominant hemisphere, this is reflected in improved calculation and language skills and, in the nondominant hemisphere, in improved sensory visuospatial processing skills and understanding of spatial orientation and navigation (Corbetta and Shulman 2002; Brownsett and Wise 2010; Friederici 2017). Abnormal asymmetries have been reported that that are associated with a range of psychiatric disorders, such as attention deficit hyperactivity disorder (ADHD; Shaw et al. 2009), autism spectrum disorder (ASD; Herbert et al. 2005), and dyslexia (Leonard et al. 2006). Investigating the asymmetries

of brain regionalization can facilitate our understanding of the physiological mechanisms behind them and enable early interventions for treatment.

However, there are limitations in this study. Although the tracking algorithms produce tractograms containing 90% of the ground truth bundles, many false positive results have also been reported (Maier-Hein et al. 2017) due to the presence of crossing fibers and to gyral bias (Eickhoff et al. 2018). Although multiple strategies have been used to reduce false connections in our study, we cannot rule out the possibility of residual false positive connections. In addition, overproduction and developmental remodeling, including a substantial elimination of synaptic spines, continues beyond adolescence (Petanjek et al. 2011). Differentiation and maturation of neuronal circuitry may also be influential factors that lead to differences in brain arealization between children and adults (Petanjek et al. 2019). In summary, it is important to complement tractography results with a combination of histological or neurophysiological methods to obtain more accurate structural connectivity results. Data from as many modalities as possible should be combined in future studies for a more comprehensive analysis to increase the certainty of the conclusions.

In summary, in this study, we used longitudinal data for the first time to create a whole brain atlas oriented toward age-specific children and explored the changes in the regionalization patterns of the developing brain as well as how they differ from those of adult regionalization patterns. For ease of use in future studies, we divided the ROIs into 2 groups based on the similarities and differences in regionalization patterns. The process of maturation of different regions of the brain in response to specific tasks in developmental processes can be better understood by considering the groups determined by partitioning. In addition, the developmental trends in inter-hemispheric lateralization of the brain also warrant more attention in future studies. Finally, if the maturation process in the highly dynamic connectivity patterns of childhood development not only increases functional plasticity but also increases the potential for experiencing psychiatric disorders (Cao et al. 2017), then an age-specific child brain atlas may contribute to a more detailed understanding of the biological mechanisms of developmental disorders and facilitate the implementation of early interventions.

Acknowledgment

The authors appreciate the English language and editing assistance of R. E. Perozzi and E. F. Perozzi.

Supplementary Material

Supplementary material is available at *Cerebral Cortex* online.

Funding

This work was supported by the following sources:

Science and Technology Innovation 2030—Brain Science and Brain-Inspired Intelligence Project of China (grant no. 2021ZD0200200); the National Natural Science Foundation of China (grant nos. 31620103905, 82151307, and 82072099); the Chinese Academy of Sciences, Science and Technology Service Network Initiative (grant no. KFJ-STS-ZDTP-078); the Science Frontier Program of the Chinese Academy of Sciences (grant no. QYZDJ-SSW-SMC019); the Beijing Municipal Science & Technology Commission (grant nos. Z161100000216152 and Z171100000117002); and the Strategic Priority Research Program of the Chinese Academy of Sciences (XDB32030200 and XDB32030207).

Conflict of interest statement: All authors declare no competing interests.

Authors' contributions

T.J. led the project and the concept design. W.L. carried out the data processing. T.J. and W.L. analyzed the data, created the figures, and wrote the manuscript. T.J., L.F., and W.S. contributed to the organization of the manuscript. Y.L., J.L., N.L. H.W., C.C., L.M. K.L., L.Q.C., M.S., and L.C provided crucial advice for the study. All of the co-authors participated in discussions of the results and revision of the manuscript.

References

Baker CM, Burks JD, Briggs RG, Sheets JR, Conner AK, Glenn CA, Sali G, McCoy TM, Battiste JD, O'Donoghue DL. A connectomic atlas of the human cerebrum—chapter 3: the motor, premotor, and sensory cortices. *Oper Neurosurg*. 2018:15(suppl_1):S75–S121.

Barrett HC. A hierarchical model of the evolution of human brain specializations. *Proc Natl Acad Sci*. 2012:109(supplement_1): 10733–10740.

Bassett DS, Wymbs NF, Porter MA, Mucha PJ, Carlson JM, Grafton ST. Dynamic reconfiguration of human brain networks during learning. *Proc Natl Acad Sci*. 2011:108(18):7641–7646.

Behrens TEJ, Johansen Berg H, Jbabdi S, Rushworth MFS, Woolrich MW. Probabilistic diffusion tractography with multiple fibre orientations: what can we gain? *NeuroImage*. 2007:34(1):144–155.

Bethlehem RAI, Seidlitz J, White SR, Vogel JW, Anderson KM, Adamson C, Adler S, Alexopoulos GS, Anagnostou E, Areces-Gonzalez A. Brain charts for the human lifespan. *Nature*. 2022:1-11:1476–4687.

Betzel RF, Byrge L, He Y, Goñi J, Zuo X-N, Sporns O. Changes in structural and functional connectivity among resting-state networks across the human lifespan. *NeuroImage*. 2014:102:345–357.

Binder JR, Desai RH, Graves WW, Conant LL. Where is the semantic system? A critical review and meta-analysis of 120 functional neuroimaging studies. *Cereb Cortex*. 2009:19(12):2767–2796.

Brownsett SLE, Wise RJS. The contribution of the parietal lobes to speaking and writing. *Cereb Cortex*. 2010:20(3):517–523.

Buckner RL, Krienen FM. The evolution of distributed association networks in the human brain. *Trends Cogn Sci*. 2013:17(12): 648–665.

Cadwell CR, Bhaduri A, Mostajo-Radji MA, Keefe MG, Nowakowski TJ. Development and arealization of the cerebral cortex. *Neuron*. 2019:103(6):980–1004.

Cao M, Huang H, He Y. Developmental connectomics from infancy through early childhood. *Trends Neurosci*. 2017:40(8):494–506.

Casey BJ, Tottenham N, Liston C, Durston S. Imaging the developing brain: what have we learned about cognitive development? *Trends Cogn Sci*. 2005:9(3):104–110.

Casey BJ, Cannonier T, Conley MI, Cohen AO, Barch DM, Heitzeg MM, Soules ME, Teslovich T, Dellarco DV, Garavan H. The adolescent brain cognitive development (ABCD) study: imaging acquisition across 21 sites. *Dev Cogn Neurosci*. 2018:32:43–54.

Cereda C, Ghika J, Maeder P, Bogousslavsky J. Strokes restricted to the insular cortex. *Neurology*. 2002:59(12):1950–1955.

Cerliani L, Thomas RM, Jbabdi S, Siero JCW, Nanetti L, Crippa A, Gazzola V, D'Arceuil H, Keysers C. Probabilistic tractography

recovers a rostrocaudal trajectory of connectivity variability in the human insular cortex. *Hum Brain Mapp*. 2012:33(9):2005–2034.
Cloutman LL, Binney RJ, Drakesmith M, Parker GJM, Lambon Ralph MA. The variation of function across the human insula mirrors its patterns of structural connectivity: evidence from in vivo probabilistic tractography. *NeuroImage*. 2012:59(4):3514–3521.
Corbetta M, Shulman GL. Control of goal-directed and stimulus-driven attention in the brain. *Nat Rev Neurosci*. 2002:3(3):201–215.
Cramér H. *Mathematical methods of statistics (PMS-9)*. Vol. 43. Princeton University Press; 1999
Cui Z, Li H, Xia CH, Larsen B, Adebimpe A, Baum GL, Cieslak M, Gur RE, Gur RC, Moore TM. Individual variation in functional topography of association networks in youth. *Neuron*. 2020:106(2): 340–353. e8.
Danon L, Diaz-Guilera A, Duch J, Arenas A. Comparing community structure identification. *J Stat Mech*. 2005:2005(09):P09008.
de Faria O, Pivonkova H, Varga B, Timmler S, Evans KA, Káradóttir RT. Periods of synchronized myelin changes shape brain function and plasticity. *Nat Neurosci*. 2021:24(11):1508–1521.
Deen B, Pitskel NB, Pelphrey KA. Three systems of insular functional connectivity identified with cluster analysis. *Cereb Cortex*. 2011:21(7):1498–1506.
Dekaban AS, Sadowsky D. Changes in brain weights during the span of human life: relation of brain weights to body heights and body weights. *Ann Neurol*. 1978:4(4):345–356.
der Kouwe V, André JW, Benner T, Salat DH, Fischl B. Brain morphometry with multiecho MPRAGE. *NeuroImage*. 2008:40(2):559–569.
Desikan RS, Ségonne F, Fischl B, Quinn BT, Dickerson BC, Blacker D, Buckner RL, Dale AM, Maguire RP, Hyman BT. An automated labeling system for subdividing the human cerebral cortex on MRI scans into gyral based regions of interest. *NeuroImage*. 2006: 31(3):968–980.
Dice LR. Measures of the amount of ecologic association between species. *Ecology*. 1945:26(3):297–302.
Dong H-M, Margulies DS, Zuo X-N, Holmes AJ. Shifting gradients of macroscale cortical organization mark the transition from childhood to adolescence. *Proc Natl Acad Sci*. 2021:118(28).
Eickhoff SB, Thomas Yeo BT, Genon S. Imaging-based parcellations of the human brain. *Nat Rev Neurosci*. 2018:19(11):672–686.
Fan L, Li H, Zhuo J, Yu Z, Wang J, Chen L, Yang Z, Chu C, Xie S, Laird AR. The human brainnetome atlas: a new brain atlas based on connectional architecture. *Cereb Cortex*. 2016:26(8):3508–3526.
Fonov VS, Evans AC, McKinstry RC, Almli CR, Collins DL. Unbiased nonlinear average age-appropriate brain templates from birth to adulthood. *NeuroImage*. 2009:(47):S102 1053–S102 8119.
Fonov V, Evans AC, Botteron K, Almli CR, McKinstry RC, Collins DL, Group Brain Development Cooperative. Unbiased average age-appropriate atlases for pediatric studies. *NeuroImage*. 2011:54(1): 313–327.
Friederici AD. Evolution of the neural language network. *Psychon Bull Rev*. 2017:24(1):41–47.
Gardner EP. Dorsal and ventral streams in the sense of touch. In: Gardner EP, Kaas JH, editors. *The Senses: A Comprehensive Reference: Somatosensation*. Oxford, UK: Elsevier, 2008:6:233–258.
Ghaziri J, Tucholka A, Girard G, Houde J-C, Boucher O, Gilbert G, Descoteaux M, Lippé S, Rainville P, Nguyen DK. The corticocortical structural connectivity of the human insula. *Cereb Cortex*. 2017:27(2):1216–1228.
Giraud AL, Price CJ. The constraints functional neuroimaging places on classical models of auditory word processing. *J Cogn Neurosci*. 2001:13(6):754–765.
Glasser MF, Sotiropoulos SN, Anthony Wilson J, Coalson TS, Fischl B, Andersson JL, Junqian X, Jbabdi S, Webster M, Polimeni JR. The minimal preprocessing pipelines for the Human Connectome Project. *NeuroImage*. 2013:80(105–124):1053–8119.
Gracia-Tabuenca Z, Moreno MB, Barrios FA, Alcauter S. Hemispheric asymmetry and homotopy of resting state functional connectivity correlate with visuospatial abilities in school-age children. *NeuroImage*. 2018:174:441–448.
Gu S, Satterthwaite TD, Medaglia JD, Yang M, Gur RE, Gur RC, Bassett DS. Emergence of system roles in normative neurodevelopment. *Proc Natl Acad Sci*. 2015:112(44):13681–13686.
Hagan JF, Shaw JS, Duncan PM. *Bright futures: American Academy of Pediatrics*, 4th ed. American Academy of Pediatrics, Elk Grove Village, IL; 2017
Harms MP, Somerville LH, Ances BM, Andersson J, Barch DM, Bastiani M, Bookheimer SY, Brown TB, Buckner RL, Burgess GC. Extending the Human Connectome Project across ages: imaging protocols for the Lifespan Development and Aging projects. *NeuroImage*. 2018:183:972–984.
Herbert MR, Ziegler DA, Deutsch CK, O'Brien LM, Kennedy DN, Filipek PA, Bakardjiev AI, James Hodgson M, Takeoka, and Nikos Makris. Brain asymmetries in autism and developmental language disorder: a nested whole-brain analysis. *Brain*. 2005:128(1):213–226.
Jelacic S, de Regt D, Weinberger E. Interactive digital MR atlas of the pediatric brain. *Radiographics*. 2006:26(2):497–501.
Johansen-Berg H, Behrens TEJ, Sillery E, Ciccarelli O, Thompson AJ, Smith SM, Matthews PM. Functional–anatomical validation and individual variation of diffusion tractography-based segmentation of the human thalamus. *Cereb Cortex*. 2005:15(1):31–39.
Johansen-Berg H, Della-Maggiore V, Behrens TEJ, Smith SM, Paus T. Integrity of white matter in the corpus callosum correlates with bimanual co-ordination skills. *NeuroImage*. 2007:36:T16–T21.
Jumah FR, Dossani RH. Neuroanatomy, cingulate cortex. In: *StatPearls*. Treasure Island (FL): StatPearls Publishing; 2019.
Kelly A, Clare M, Di Martino A, Uddin LQ, Shehzad Z, Gee DG, Reiss PT, Margulies DS, Xavier Castellanos F, Milham MP. Development of anterior cingulate functional connectivity from late childhood to early adulthood. *Cereb Cortex*. 2009:19(3):640–657.
Koelkebeck K, Miyata J, Kubota M, Kohl W, Son S, Fukuyama H, Sawamoto N, Takahashi H, Murai T. The contribution of cortical thickness and surface area to gray matter asymmetries in the healthy human brain. *Hum Brain Mapp*. 2014:35(12): 6011–6022.
Koenigs M, Barbey AK, Postle BR, Grafman J. Superior parietal cortex is critical for the manipulation of information in working memory. *J Neurosci*. 2009:29(47):14980–14986.
Kropf E, Syan SK, Minuzzi L, Frey BN. From anatomy to function: the role of the somatosensory cortex in emotional regulation. *Braz J Psychiatry*. 2018:41(3):261–269.
Lafer-Sousa R, Conway BR. Parallel, multi-stage processing of colors, faces and shapes in macaque inferior temporal cortex. *Nat Neurosci*. 2013:16(12):1870–1878.
Lancichinetti A, Fortunato S, Kertész J. Detecting the overlapping and hierarchical community structure in complex networks. *New J Phys*. 2009:11(3):033015.
Lenroot RK, Giedd JN. Brain development in children and adolescents: insights from anatomical magnetic resonance imaging. *Neurosci Biobehav Rev*. 2006:30(6):718–729.
Leonard C, Eckert M, Given B, Virginia B, Eden G. Individual differences in anatomy predict reading and oral language impairments in children. *Brain*. 2006:129(12):3329–3342.
Li W, Shi W, Wang H, Li J, Cui Y, Li K, Cheng L, Lu Y, Liang M, Chu C. Anatomical connectivity profile development constrains medial-lateral topography in the dorsal prefrontal cortex. *Sci Adv*. 2022: bioRxiv.

Liang X, Zhao C, Jin X, Jiang Y, Yang L, Chen Y, Gong G. Sex-related human brain asymmetry in hemispheric functional gradients. *NeuroImage*. 2021:229:117761.

Loveless B. *Learning to read to read to learn. Education corner: myth or reality*; 2020

Luders E, Narr KL, Thompson PM, Rex DE, Jancke L, Toga AW. Hemispheric asymmetries in cortical thickness. *Cereb Cortex*. 2006:16(8):1232–1238.

Maier-Hein KH, Neher PF, Houde J-C, Côté M-A, Garyfallidis E, Zhong J, Chamberland M, Yeh F-C, Lin Y-C, Ji Q. The challenge of mapping the human connectome based on diffusion tractography. *Nat Commun*. 2017:8(1):1–13.

Makuuchi M, Bahlmann J, Anwander A, Friederici AD. Segregating the core computational faculty of human language from working memory. *Proc Natl Acad Sci*. 2009:106(20):8362–8367.

Mars RB, Verhagen L, Gladwin TE, Neubert F-X, Sallet J, Rushworth MFS. Comparing brains by matching connectivity profiles. *Neurosci Biobehav Rev*. 2016:60:90–97.

Molfese PJ, Glen D, Mesite L, Cox RW, Hoeft F, Frost SJ, Mencl WE, Pugh KR, Bandettini PA. The Haskins pediatric atlas: a magnetic-resonance-imaging-based pediatric template and atlas. *Pediatr Radiol*. 2021:51(4):628–639.

Nomi JS, Farrant K, Damaraju E, Rachakonda S, Calhoun VD, Uddin LQ. Dynamic functional network connectivity reveals unique and overlapping profiles of insula subdivisions. *Hum Brain Mapp*. 2016:37(5):1770–1787.

Ossmy O, Mukamel R. Activity in superior parietal cortex during training by observation predicts asymmetric learning levels across hands. *Sci Rep*. 2016:6(1):1–9.

Passingham RE, Stephan KE, Kötter R. The anatomical basis of functional localization in the cortex. *Nat Rev Neurosci*. 2002:3(8):606–616.

Penhune VB, Zatorre RJ, MacDonald JD, Evans AC. Interhemispheric anatomical differences in human primary auditory cortex: probabilistic mapping and volume measurement from magnetic resonance scans. *Cereb Cortex*. 1996:6(5):661–672.

Petanjek Z, Judaš M, Šimić G, Rašin MR, Uylings HBM, Rakic P, Kostović I. Extraordinary neoteny of synaptic spines in the human prefrontal cortex. *Proc Natl Acad Sci*. 2011:108(32):13281–13286.

Petanjek Z, Sedmak D, Džaja D, Hladnik A, Rašin MR, Jovanov-Milosevic N. The protracted maturation of associative layer IIIC pyramidal neurons in the human prefrontal cortex during childhood: a major role in cognitive development and selective alteration in autism. *Front Psychiatry*. 2019:10:122 1664–122 0640.

Qin S, Young CB, Supekar K, Uddin LQ, Menon V. Immature integration and segregation of emotion-related brain circuitry in young children. *Proc Natl Acad Sci*. 2012:109(20):7941–7946.

Renteria ME. Cerebral asymmetry: a quantitative, multifactorial, and plastic brain phenotype. *Twin Res Hum Genet*. 2012:15(3):401–413.

Roberts JA, Perry A, Roberts G, Mitchell PB, Breakspear M. Consistency-based thresholding of the human connectome. *NeuroImage*. 2017:145:118–129.

Rousseeuw PJ. Silhouettes: a graphical aid to the interpretation and validation of cluster analysis. *J Comput Appl Math*. 1987:20:53–65.

Saygin ZM, Osher DE, Norton ES, Youssoufian DA, Beach SD, Feather J, Gaab N, Gabrieli JDE, Kanwisher N. Connectivity precedes function in the development of the visual word form area. *Nat Neurosci*. 2016:19(9):1250–1255.

Shaw P, Lalonde F, Lepage C, Rabin C, Eckstrand K, Sharp W, Greenstein D, Evans A, Giedd JN, Rapoport J. Development of cortical asymmetry in typically developing children and its disruption in attention-deficit/hyperactivity disorder. *Arch Gen Psychiatry*. 2009:66(8):888–896.

Shum J, Hermes D, Foster BL, Dastjerdi M, Rangarajan V, Winawer J, Miller KJ, Parvizi J. A brain area for visual numerals. *J Neurosci*. 2013:33(16):6709–6715.

Sydnor VJ, Larsen B, Bassett DS, Alexander-Bloch A, Fair DA, Liston C, Mackey AP, Milham MP, Pines A, Roalf DR. Neurodevelopment of the association cortices: patterns, mechanisms, and implications for psychopathology. *Neuron*. 2021:109(18):2820–2846.

Taing AS, Mundy ME, Ponsford JL, Spitz G. Temporal lobe activation during episodic memory encoding following traumatic brain injury. *Sci Rep*. 2021:11(1):1–12.

Thompson PM, Giedd JN, Woods RP, MacDonald D, Evans AC, Toga AW. Growth patterns in the developing brain detected by using continuum mechanical tensor maps. *Nature*. 2000:404(6774):190–193.

Toga AW, Thompson PM. Mapping brain asymmetry. *Nat Rev Neurosci*. 2003:4(1):37–48.

Tzourio-Mazoyer N. Intra-and inter-hemispheric connectivity supporting hemispheric specialization. *Micro-, meso-and macro-connectomics of the brain*. 2016:129–146.

Wasserthal J, Neher P, Maier-Hein KH. TractSeg-Fast and accurate white matter tract segmentation. *NeuroImage*. 2018:183:239–253.

Wierenga LM, Langen M, Oranje B, Durston S. Unique developmental trajectories of cortical thickness and surface area. *NeuroImage*. 2014:87:120–126.

Yakovlev PI, Lecours A-R, Minkowski A, Davis FA. Regional development of the brain in early life. 1967.

Yeo BT, Krienen FM, Sepulcre J, Sabuncu MR, Lashkari D, Hollinshead M, Roffman JL, Smoller JW, Zöllei L, Polimeni JR, et al. The organization of the human cerebral cortex estimated by intrinsic functional connectivity. *J Neurophysiol*. 2011:106(3):1125–1165.

Yushkevich PA, Piven J, Hazlett HC, Smith RG, Ho S, Gee JC, Gerig G. User-guided 3D active contour segmentation of anatomical structures: significantly improved efficiency and reliability. *NeuroImage*. 2006:31(3):1116–1128.

Zhu J, Zhang H, Chong Y-S, Shek LP, Gluckman PD, Meaney MJ, Fortier MV, Qiu A. Integrated structural and functional atlases of Asian children from infancy to childhood. *NeuroImage*. 2021:245:118716.